Article

Cell Reports

Enhanced Transcriptional Activity and Mitochondrial Localization of STAT3 Co-induce Axon Regrowth in the Adult Central Nervous System

Graphical Abstract

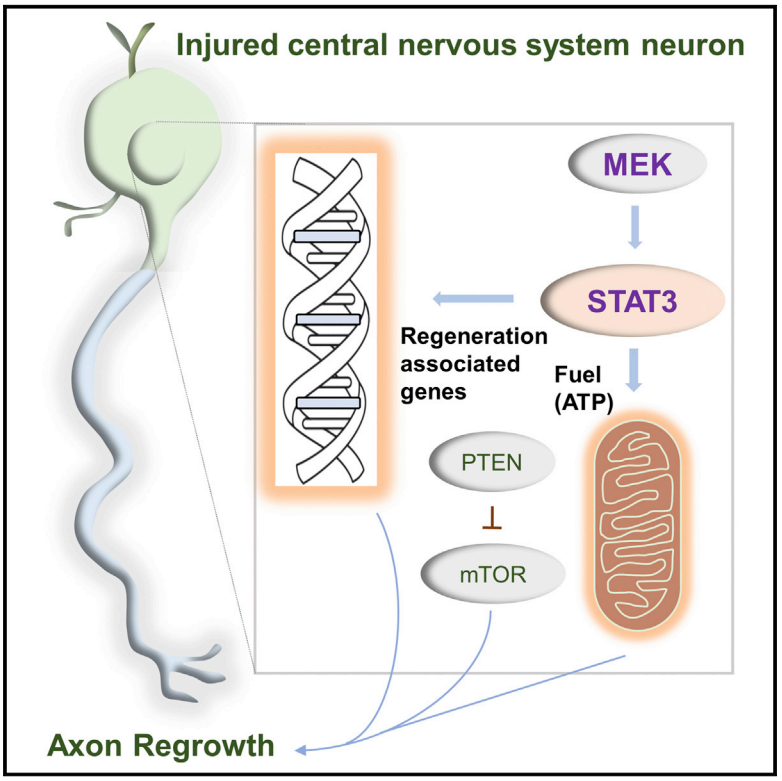

Authors

Xueting Luo, Marcio Ribeiro, Eric R. Bray, ..., John L. Bixby, Vance P. Lemmon, Kevin K. Park

Correspondence

kpark@miami.edu

In Brief

Luo et al. provide mechanistic insights into how STAT3 induces axon regeneration and sprouting after injury. They demonstrate that exploiting STAT3′s effects in combination with modulation of MEK and PTEN promotes extensive CNS axon regrowth.

Highlights

- STAT3 shifts to distinct cellular regions in CNS neurons upon cytokine stimulation
- STAT3′s transcriptional activity and mitochondrial localization co-induce regeneration
- MEK enhances STAT3 functions and localization and potentiates axon regeneration
- Modulation of STAT3, MEK, and PTEN promotes extensive axon growth and sprouting

Luo et al., 2016, Cell Reports *15*, 398–410
April 12, 2016
http://dx.doi.org/10.1016/j.celrep.2016.03.029

CellPress

OPEN ACCESS
CellPress

Cell Reports
Article

Enhanced Transcriptional Activity and Mitochondrial Localization of STAT3 Co-induce Axon Regrowth in the Adult Central Nervous System

Xueting Luo,[1,3] Marcio Ribeiro,[1] Eric R. Bray,[1] Do-Hun Lee,[1] Benjamin J. Yungher,[1] Saloni T. Mehta,[1] Kinjal A. Thakor,[1] Francisca Diaz,[2] Jae K. Lee,[1] Carlos T. Moraes,[2] John L. Bixby,[1] Vance P. Lemmon,[1] and Kevin K. Park[1,*]
[1]Department of Neurological Surgery, Miami Project to Cure Paralysis
[2]Department of Neurology
University of Miami Miller School of Medicine, Miami, FL 33136, USA
[3]Present address: Department of Ophthalmology, Shanghai First People's Hospital, Shanghai Jiao Tong University School of Medicine; Shanghai Key Laboratory of Fundus Disease, 100 Hai Ning Road, Shanghai 200080, China
*Correspondence: kpark@miami.edu
http://dx.doi.org/10.1016/j.celrep.2016.03.029

SUMMARY

Signal transducer and activator of transcription 3 (STAT3) is a transcription factor central to axon regrowth with an enigmatic ability to act in different subcellular regions independently of its transcriptional roles. However, its roles in mature CNS neurons remain unclear. Here, we show that along with nuclear translocation, STAT3 translocates to mitochondria in mature CNS neurons upon cytokine stimulation. Loss- and gain-of-function studies using knockout mice and viral expression of various STAT3 mutants demonstrate that STAT3′s transcriptional function is indispensable for CNS axon regrowth, whereas mitochondrial STAT3 enhances bioenergetics and further potentiates regrowth. STAT3′s localization, functions, and growth-promoting effects are regulated by mitogen-activated protein kinase kinase (MEK), an effect further enhanced by *Pten* deletion, leading to extensive axon regrowth in the mouse optic pathway and spinal cord. These results highlight CNS neuronal dependence on STAT3 transcriptional activity, with mitochondrial STAT3 providing ancillary roles, and illustrate a critical contribution for MEK in enhancing diverse STAT3 functions and axon regrowth.

INTRODUCTION

The central nervous system (CNS) is composed of distinct neuronal types, most of which fail to regenerate after injury. While significant progress has been made in identifying genes involved in regulating axon regrowth, the mechanisms underlying regeneration failure remain elusive (Case and Tessier-Lavigne, 2005; Cregg et al., 2014; Huebner and Strittmatter, 2009; Sun and He, 2010). The interleukin-6 (IL-6) family of cytokines promotes axon regeneration (Cafferty et al., 2004; Cao et al., 2006; Leaver et al., 2006; Leibinger et al., 2009; Müller et al., 2009; Pernet et al., 2013a; Zigmond, 2011), and identification of downstream molecules that mediate cytokines' actions in neurons has provided some insights into signaling pathways and neuron-intrinsic molecular mechanisms that regulate axon regeneration process. The IL6 family of cytokines activates many signaling molecules, triggered by dimerization of gp130 and phosphorylation of Janus kinases (JAKs). These proteins serve as docking sites for several adaptors that link the receptor to signal transducer and activator of transcription (STAT), mitogen activated protein (MAP) kinases, and PI3K/Akt (Ernst and Jenkins, 2004). In addition, they activate other central regulators of cell growth including mammalian target of rapamycin (mTOR), nuclear factor κB (NF-κB), and Yes-associated protein (YAP) (Gallagher et al., 2007; Saleh et al., 2013; Smith et al., 2009; Taniguchi et al., 2015). However, activating these target modules individually in neurons results in only limited regeneration (Pernet et al., 2005, 2013b), indicative of multifaceted mechanisms that mediate axon regeneration.

Signal transducer and activator of transcription 3 (STAT3) is a transcription factor involved in many biological processes. Genetic and pharmacological inhibition of STAT3 reduces axon regeneration both in central and peripheral nervous systems (Bareyre et al., 2011; Leibinger et al., 2013), demonstrating its role in promoting axon regeneration. Most of STAT3′s functions are attributed to transcriptional regulation. However, recent studies have demonstrated that STAT3 can also function outside the nucleus; STAT3 proteins are found in the mitochondria where they locally regulate metabolic functions in non-neuronal cells (Gough et al., 2009; Wegrzyn et al., 2009). In vitro cytoplasmic STAT3 is required for ciliary neurotrophic factor (CNTF)-induced axon growth in embryonic neurons (Selvaraj et al., 2012), and mitochondrially localized STAT3 promotes neurite outgrowth in PC12 cells (Zhou and Too, 2011). Intriguingly, these studies indicated that the transcriptional activity of STAT3 is not required for these axon growth-promoting effects. Conversely, both nuclear and cytoplasmic STAT3 are required to induce axon growth in peripheral neurons (Pellegrino and Habecker, 2013), indicating that the mechanisms by which STAT3 promotes axon growth

might be different among distinct cell types and under different conditions. It is unclear whether STAT3′s transcription-independent functions are broadly involved in different systems and whether they play a role in axon regeneration in the mature CNS. Here, we examine STAT3′s transcription-independent roles in adult CNS neurons. Our study shows that STAT3 localizes to both nucleus and mitochondria in adult retinal ganglion cells (RGCs) in response to cytokine, and enhancing STAT3′s transcription activity and localization to mitochondria together improves optic nerve regeneration. Further, STAT3′s transcription activity, mitochondrial localization, and growth promoting effects are enhanced by mitogen-activated protein kinase kinase (MEK), an effect further enhanced by *Pten* deletion with extensive axon regrowth in mouse optic pathway and spinal cord. These results establish STAT3′s transcription-dependent and -independent contributions to promoting axon regrowth in the mature CNS and suggest that MEK enhancement of STAT3′s versatile functions is integral in this function.

RESULTS

CNTF Induces Phosphorylation and Translocation of STAT3 to Distinct Subcellular Regions in CNS Neurons: MEK-Dependent Translocation of STAT3 in Mitochondria

To gain insights into STAT3′s mode of action and its potential regulators in promoting axon regeneration in mature CNS neurons, we examined activation status of STAT3 and several other key factors linked to cytokine-induced cell growth (Ernst and Jenkins, 2004; Gallagher et al., 2007; Taniguchi et al., 2015) in postmitotic postnatal (P) 3 cortical neurons following CNTF treatment. Elevating CNTF levels promotes axon regeneration in vivo and increases neurite outgrowth in vitro (Gallagher et al., 2007; Leaver et al., 2006; Pernet et al., 2013a; Selvaraj et al., 2012; Smith et al., 2009; Sun et al., 2011). As expected, addition of recombinant CNTF (rCNTF) led to rapid activation of STAT3 (Figure S1); the levels of STAT3 phosphorylation at serine 727 (S727) and tyrosine 705 (Y705) remained elevated for at least 20 hr after adding rCTNF. Similarly, the level of ERK phosphorylation rapidly increased before returning to the basal level. The level of phosphorylated S6 (pS6), an indicator of mTOR activity, moderately increased in the absence of Akt activation. No obvious change was detected for IκBα, YAP, and β-catenin (Figure S1). To further examine STAT3′s mode of action in CNS neurons, we investigated STAT3 expression in adult RGCs. In response to growth factors, STAT3 is phosphorylated at Y705 and S727, binds to DNA, and regulates transcription. Consistently, immunohistochemistry shows that intravitreal injection of adeno-associated virus (AAV) expressing the secretable form of CNTF (Leaver et al., 2006) (AAV-CNTF), known to promote RGC axon regeneration (Leaver et al., 2006; Pernet et al., 2013a), elevates the levels of phosphorylated STAT3 (pSTAT3) at both Y705 and S727 in RGCs (Figure 1A). Notably, however, we observed that the cellular localization patterns of pSTAT3(Y705) and pSTAT3(S727) are distinct; pSTAT3(Y705) seems to localize exclusively in the nucleus whereas pSTAT3(S727) is also found in the cytoplasm and RGC processes (Figure 1A). Are there functional roles for STAT3 proteins located outside RGC nucleus? Since past studies have shown mitochondrial STAT3′s ability to promote neurite growth, and translocation of STAT3 to mitochondria requires phosphorylation at S727 (Gough et al., 2009; Tammineni et al., 2013; Wegrzyn et al., 2009), we examined whether STAT3 translocates to mitochondria in RGCs after CNTF treatment. First, we used confocal microscopy and quantified the levels of pSTAT3(S727) co-localizing with the mitochondrial protein ATP synthase β (ATPsynβ). Compared to controls, there was a significant increase in the pSTAT3(S727)/ATPsynβ co-localization in RGCs in CNTF-treated retina (Figures 1B and 1C), indicative of STAT3s's presence in RGC mitochondria. Additionally, we examined STAT3′s subcellular localization using ascorbate peroxidase (APEX) protein-tagging technique. APEX is a monomeric peroxidase that endures strong electron microscope fixation, preserving ultrastructural details (Martell et al., 2012). At electron microscope (EM) level, STAT3 is detected in inner mitochondrial membrane in CNTF-treated cortical neurons (Figure 1D). Since phosphorylation at the S727 residue is critical for STAT3 mitochondrial localization (Gough et al., 2009; Tammineni et al., 2013), and CNTF induces activation of ERK (Figure S1), a protein kinase shown to cause S727 phosphorylation (Zhou and Too, 2011), we examined whether MEK (the upstream activator of ERK) induces STAT3 phosphorylation and translocation to mitochondria. Pharmacological MEK inhibitors almost completely blocked ERK phosphorylation and CNTF-mediated STAT3 S727 phosphorylation in cortical neurons. In contrast, pSTAT3 (Y705) level was not affected by these inhibitors (Figure 1E). Additionally, subcellular fractionation reveals that total STAT3 and pSTAT3(S727) levels in the mitochondria increased ~2- and 2.5-fold, respectively, after CNTF treatment (Figures 1F and 1G). Increases in the level of total STAT3 (but not pSTAT3(S727)) were also detected in the nuclear fraction but only after exposing the film for a prolonged period (Figure 1F). Refamitinib (MEK inhibitor) significantly reduced the amounts of pSTAT3(S727) and total STAT3 in the mitochondria (Figures 1F and 1G). Together, these data demonstrate that CNTF promotes phosphorylation and translocation of STAT3 to both the nuclei and mitochondria in post-mitotic CNS neurons and suggests that mitochondrial presence of STAT3 is MEK-dependent.

DNA Binding Domain of STAT3 Is Essential for CNTF-Induced RGC Axon Regeneration

Translocation of STAT3 to different subcellular locations in RGCs raises a question of the extent to which the transcriptional activity-dependent (nuclear) and -independent functions of STAT3 contribute to promoting CNS axon regeneration. To examine this question, we designed an optic nerve regeneration experiment using *Stat3*$^{f/f}$ mice crossed to *R26-tdTomato* reporter (*Stat3*$^{f/f}$*;R26-tdTomato*) in which *Stat3* null RGCs can be created and STAT3 expression reconstituted with AAV2 expressing various STAT3 mutants (Figure 2A). Intravitreal injection of AAV-Cre in this mouse line results in concomitant *Stat3* deletion and tdTomato-labeling in transduced cells. We injected AAV-Cre together with AAV expressing either wild-type STAT3 (STAT3wt) or DNA-binding mutant version of STAT3 (STAT3dbm) (Table S1) (Bromberg et al., 1998, 1999; Horvath et al., 1995) in *Stat3*$^{f/f}$*;R26-tdTomato* mice. Five days later, animals received optic nerve

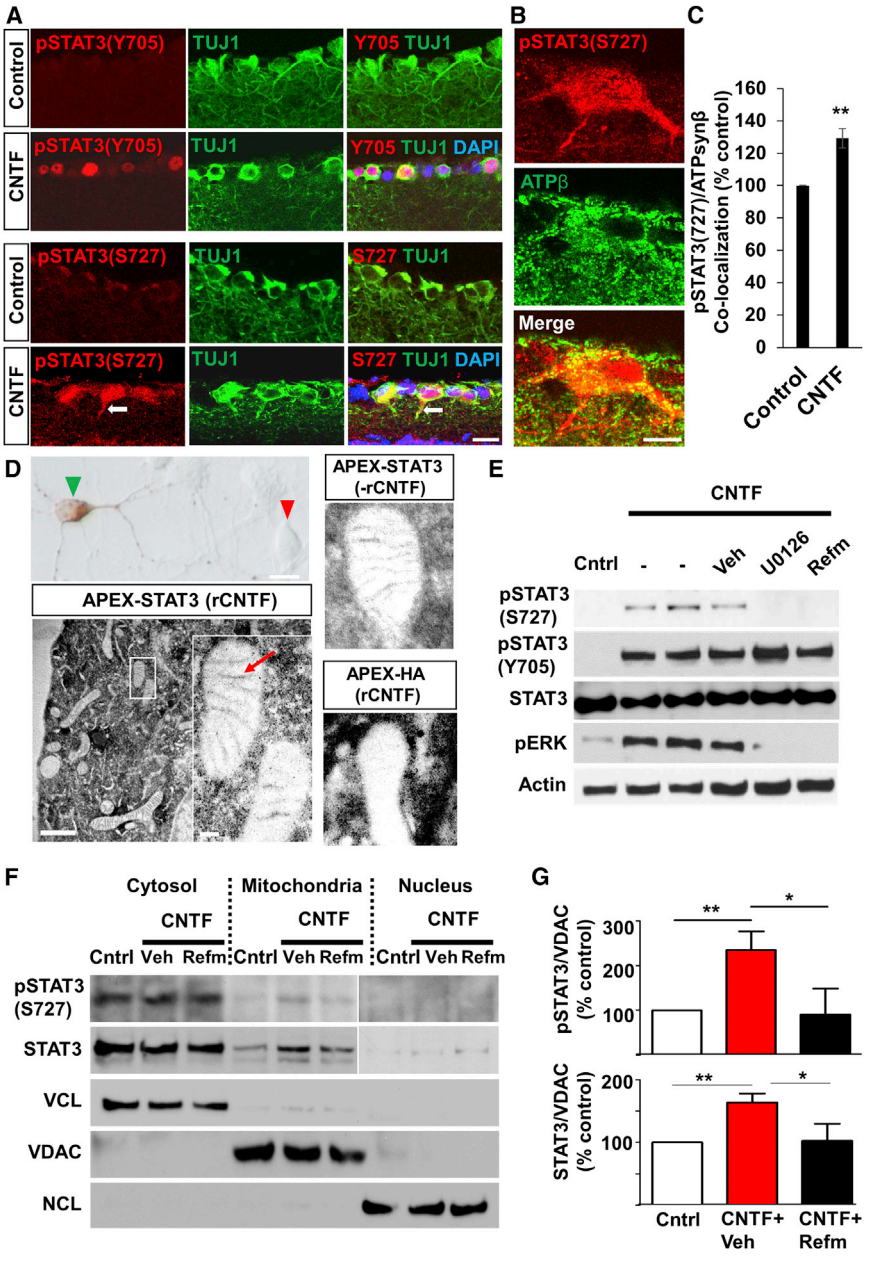

Figure 1. CNTF Induces Phosphorylation and Translocation of STAT3 Proteins to Distinct Subcellular Regions: MEK-Dependent Mitochondrial Translocation

(A) Retinal sections showing the levels of pSTAT3(Y705) and pSTAT3(S727) immunoreactivity (red) in RGCs (i.e., labeled with the TUJ1 antibody, green) 2 weeks following intravitreal AAV-GFP ("control") or AAV-CNTF injection ("CNTF"). DAPI in blue. Arrow, RGC process. Scale bar, 20 μm.

(B) Single plane confocal image showing co-labeling of mitochondrial protein ATPsynβ and pSTAT3(S727) in RGCs in AAV-CNTF-treated retina. Scale bar, 20 μm.

(C) Quantification of pSTAT3(S727) and ATPsynβ co-localization. For each retina, 15–20 individual RGCs were measured, and three retinas were analyzed per group. Value of the control group (AAV-GFP) is represented as 100%. **$p < 0.01$ by unpaired Student's t test.

(D) Upper left: bright field image showing a P3 rat cortical neuron transfected with APEX-STAT3, (green arrow head) and an untransfected cell (red arrow head). Bottom left: electron micrographs of a neuron transfected with APEX-STAT3 treated with recombinant CNTF (rCNTF; 50 ng/ml); the inset is a magnification of the white boxed area, showing mitochondria. Upper right: APEX-STAT3 without rCNTF. Bottom right: HA-APEX with rCNTF. DAB signal is detected in the inner membrane (red arrow) of mitochondria in APEX-STAT3 cells. On the other hand, while DAB signal is found throughout the cytoplasm, it is not detected in the mitochondria of HA-APEX cells. Scale bars, low magnification, 1 μm; inset, 100 nm.

(E) Western blot of P3 rat cortical neurons under various conditions; no treatment, treated with rCNTF (50 ng/ml) alone or with MEK inhibitors U0126 (5 μM) or refamitinib (Refm, 5 μM), or vehicle (Veh, DMSO) for 1 hr. The control ("cntrl") group received neither rCNTF nor MEK inhibitors.

(F) Representative western blot of fractionation-derived nuclear, cytosolic, and mitochondrial proteins from rat P3 cortical neurons showing the levels of STAT3 protein expression 4 hr after rCNTF (50 ng/ml). Total STAT3 and pSTAT3(S727) are increased in the mitochondria after rCNTF. Increases in the level of total STAT3 (but not pSTAT3(S727)) were also detected; data shown are result of 15-s exposure for the cytosol and mitochondrial fractionations and 1-min exposure for the nuclear fraction. Voltage-dependent anion channel (VDAC) mitochondrial marker, nucleolin (NCL) nuclear marker, and vinculin (VCL) cytosolic marker were used to verify the relative purity of fractionated proteins.

(G) Densitometric quantification of mitochondrial STAT3 levels in western blot normalized against VDAC. Both the total and pSTAT3(S727) protein levels are increased in mitochondria after rCNTF treatment, an effect that was reduced by refamitinib. Value for the control group is represented as 100%. Values are means obtained from at least six biological replicates. *$p < 0.05$, **$p < 0.01$ by one-way ANOVA followed by Dunnett's test.

See also Figure S1.

crush. This injection scheme (Figure 2A) allows the onset of *Stat3* ablation in adult RGCs without the tdTomato presence in the optic nerve before the injury (Sun et al., 2011), thus allowing tdTomato labeling only in regenerating and not in degenerated axons. Immediately after injury, animals also received injection of either AAV-GFP or AAV-CNTF. At 19 days post-injury, we examined the extent of tdTomato-labeled (i.e., *Stat3* knockout [KO]) regenerating axons. Consistent with the previous studies (Park et al., 2008; Sun et al., 2011), AAV-Cre injection infected the majority of RGCs (~90%) as evident by Cre and tdTomato immunoreactivity in the *R26-tdTomato* mice (Figure 2B). In mice without *Stat3* deletion, AAV-CNTF resulted in significant RGC axon regeneration (Figures 2C and 2D). *Stat3* deletion completely eliminated CNTF-induced regeneration. Reconstituting

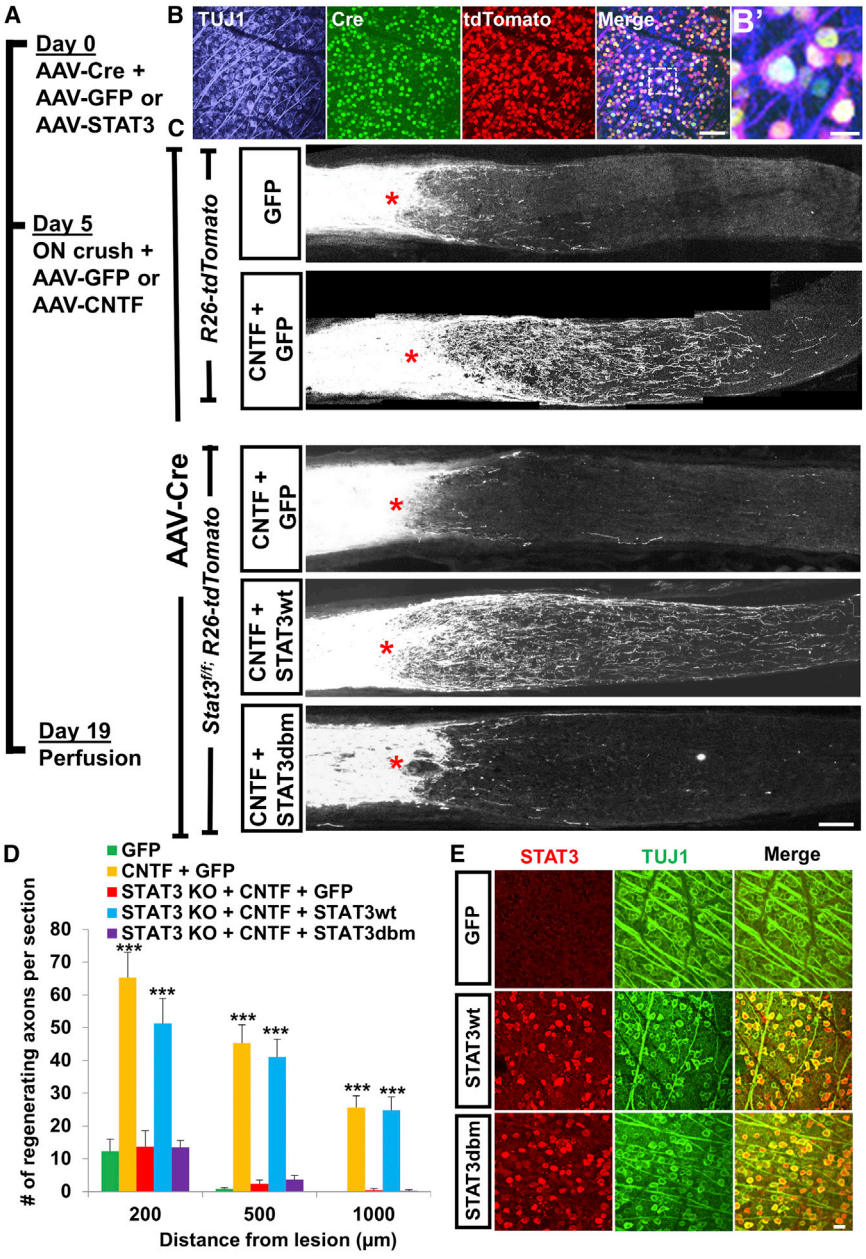

Figure 2. DNA Binding Domain of STAT3 Is Essential for CNTF-Induced RGC Axon Regeneration

(A) Time line of STAT3 in vivo rescue experiment. AAV-Cre together with either AAV-GFP or AAV vectors carrying different versions of STAT3 were injected intravitreally in *R26-tdTomato* or *Stat3*$^{f/f}$*;R26-tdTomato* mice. Five days later, animals received optic nerve crush plus AAV-GFP or AAV-CNTF injection.

(B) Whole-mount retinal staining showing Cre, tdTomato, and TUJ1 immunoreactivity 2 weeks after AAV-Cre injection in a *R26-tdTomato* mouse. Scale bar, 100 μm.

(B′) Higher magnification of the boxed area in (B). Scale bar, 20 μm.

(C) Representative optic nerve sections showing the degree of axon regeneration following various treatments. Axons are labeled with tdTomato via Cre recombination in *Stat3*$^{f/f}$*;R26-tdTomato* or *R26-tdTomato* mice. STAT3wt, but not STAT3dbm, rescues AAV-CNTF-induced regeneration. Red asterisks, lesion site. Scale bar, 100 μm.

(D) Quantification of tdTomato-labeled regenerating axons in various animal groups; "GFP," AAV-Cre/AAV-GFP co-injected *R26-tdTomato* mice. "CNTF + GFP," AAV-Cre/AAV-GFP co-injected *R26-tdTomato* mice with AAV-CNTF injection at the time of injury. "STAT3 KO + CNTF + GFP," AAV-Cre/AAV-GFP co-injected *Stat3*$^{f/f}$*;R26-tdTomato* mice with AAV-CNTF injection at the time of injury. "STAT3 KO + CNTF + STAT3wt," AAV-Cre and AAV-STAT3wt co-injected *Stat3*$^{f/f}$*; R26-tdTomato* mice with AAV-CNTF injection at the time of injury. "STAT3 KO + CNTF + STAT3dbm," AAV-Cre and AAV-STAT3dbm co-injected *Stat3*$^{f/f}$*;R26-tdTomato* mice with AAV-CNTF injection at the time of injury. n = 5 animals/group. ***$p < 0.001$ compared to the "GFP group" using two-way repeated-measures ANOVA followed by Bonferroni post-test.

(E) Whole-mount retinal immunohistochemistry showing transduction efficacy of AAV- STAT3wt and AAV-STAT3dbm in RGCs. C57BL/6 mice received intravitreal AAV injection and the tissues were analyzed 2 weeks later. Approximately 60% of RGCs (TUJ1$^+$, green) are transduced as evident by STAT3 immunoreactivity (red) compared to undetectable STAT3 seen in the AAV-GFP injected retina. Scale bar, 20 μm.

See also Figure S2 and Table S1.

Stat3 KO-RGCs with STAT3wt (i.e., with AAV-STAT3wt) rescued CNTF-induced regeneration. In contrast, AAV-STAT3dbm failed to rescue regeneration (Figures 2C and 2D). Using qRT-PCR, we validated that STAT3dbm is transcriptionally inactive as it does not increase the expression of *Socs3* (data not shown), a prominent STAT3 target gene. RGC transduction efficiency was ~60% for both AAV-STAT3wt and AAV-STAT3dbm (Figure 2E). Additionally, we assessed RGC survival. The increase in RGC survival induced by CNTF is reduced by *Stat3* deletion. Reconstitution with STAT3wt, but not with STAT3dbm, rescued CNTF's RGC survival effect (Figures S2A and S2B). Together, these data establish that the DNA binding domain of STAT3 is essential for CNTF-induced RGC axon regeneration, strongly suggesting a requirement for transcriptional activity.

Mitochondrial STAT3′s Involvement in CNS Axon Regeneration

While our data point to a requirement for STAT3′s transcriptional function, distribution of phosphorylated STAT3 proteins in the RGC cytoplasm suggests that non-nuclear STAT3 may additionally facilitate regeneration. To directly evaluate the role of mitochondrial STAT3 in RGC axon regeneration, we generated AAV expressing the DNA binding mutant form of STAT3, that also contains a mitochondrial targeting sequence (STAT3mts) taken

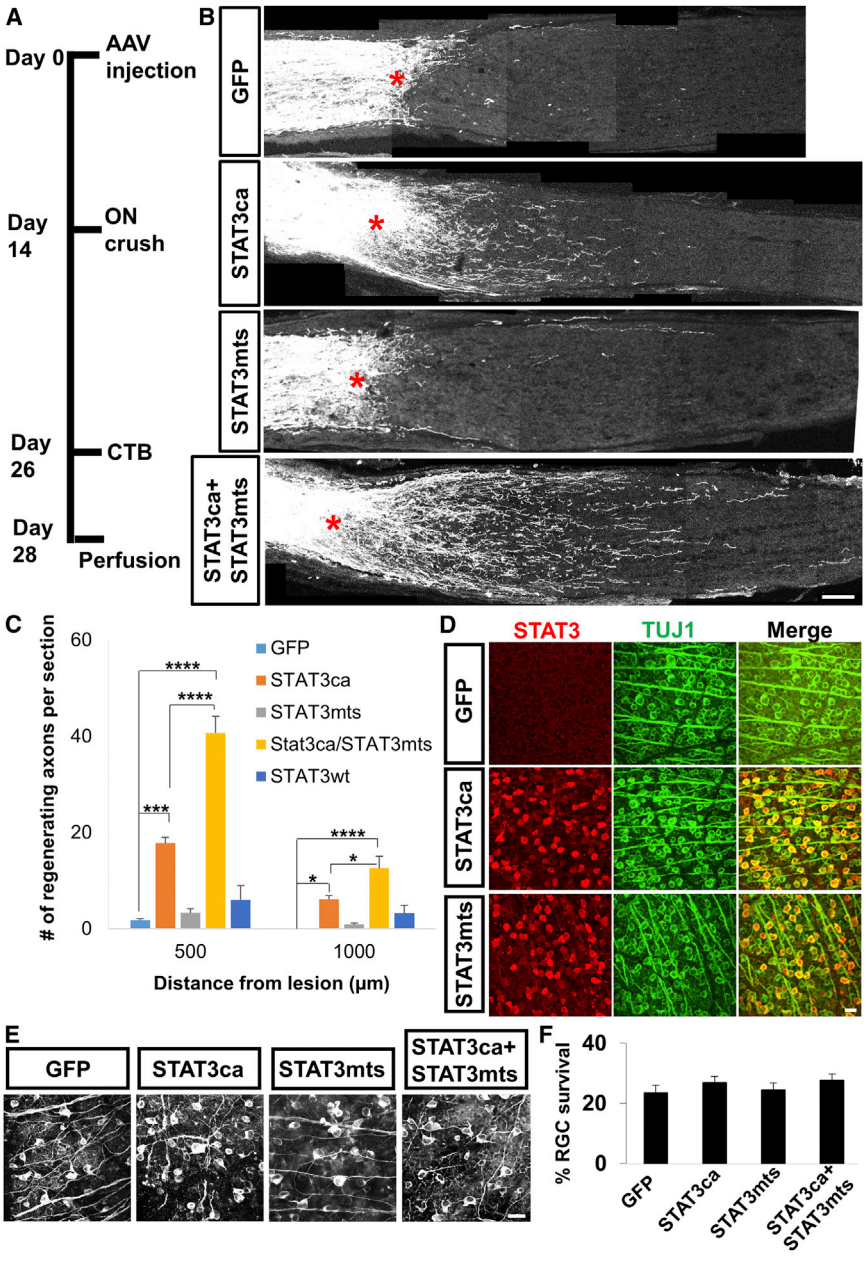

Figure 3. Site-Specific STAT3 Effects: Mitochondrial STAT3 Facilitates Axon Regeneration in the Presence of STAT3ca

(A) Time line of the experiment.

(B) Representative optic nerve sections showing the degree of axon regeneration in animals treated with either AAV-GFP, AAV-STAT3ca, or AAV-STAT3mts alone, or AAV-STAT3ca/AAV-STAT3mts together 2 weeks prior to injury. Axons are anterogradely labeled by CTB. Red asterisks, lesion site. Scale bar, 100 μm.

(C) Quantification of CTB-labeled regenerating axons in various animal groups (AAV-GFP, AAV-STAT3wt, AAV-STAT3ca, or AAV-STAT3mts alone, or AAV-STAT3ca/AAV-STAT3mts). n = 4–7 animals/group. *p < 0.05, ***p < 0.001, ****p < 0.0001 by two-way repeated-measures ANOVA followed by Bonferroni post-test.

(D) Whole-mount retinal immunohistochemistry showing transduction efficacy of AAV-STAT3ca and AAV-STAT3mts. AAV was injected in adult WT mice, and retinas were removed 2 weeks post-injection. Approximately 60% of RGCs (TUJ1$^+$, green) are transduced as evident by STAT3 immunoreactivity (red) compared to undetectable STAT3 seen in the AAV-GFP injected retina. Scale bar, 20 μm.

(E) Representative retinal whole-mount images with TUJ1 staining at 2 weeks post-injury in animals subjected to either AAV-GFP, AAV-STAT3ca or AAV-STAT3mts alone, or AAV-STAT3ca/AAV-STAT3mts. Scale bar, 20 μm.

(F) Quantification of RGC survival. Values are represented as the percentage of the contralateral uninjured retina. n = 6–7 animals/group.

See also Figures S2–S4 and Table S1.

from the cytochrome c oxidase subunit VIII gene (Szczepanek et al., 2011). AAV-STAT3mts alone failed to increase regeneration significantly compared to the GFP controls (Figures 3A–3C). It was previously shown that the constitutively active form of STAT3 proteins (STAT3ca) dimerizes and translocates to the nucleus, and overexpression of STAT3ca promotes axon regeneration (Pernet et al., 2013b). Consistently, we observed that AAV-STAT3ca increases regeneration (Figures 3B and 3C). AAV-STAT3wt alone led to some increase in regeneration, but this was statistically insignificant (Figure 3C). Interestingly, co-injection of AAV-STAT3mts with AAV-STAT3ca (but not with AAV-STAT3wt; data not shown) resulted in further enhancement in regeneration compared to the AAV-STAT3ca group (Figure 3C). RGC transduction efficiency was similar for these AAV viruses carrying different forms of STAT3, ~60% (Figure 3D). The improved regeneration seen after STAT3ca and STAT3mts combination could be due to separate pools of virally expressed STAT3 in the nucleus and mitochondria, acting cooperatively. Alternatively, it could occur if the concentration of virally expressed STAT3 proteins was somewhat higher in the double compared to each single AAV group. This is unlikely, as the various animal groups received equivalent final titers of each AAV (see Experimental Procedures). Moreover, we observed that overexpressed STAT3ca is detected predominantly in the nuclear and cytosolic fractions and not in the mitochondrial fraction. Conversely, overexpressed STAT3mts is localized mostly in the mitochondrial and not in the nuclear fraction (Figure S2C), indicating that the enhanced regeneration in the double AAV group is due to virally expressed STAT3 acting in different cellular compartments. Furthermore, we examined RGC survival and found no difference among the animal groups indicating that the enhanced regeneration is not due to differences in cell survival (Figures 3E and 3F). Together, these data indicate that

differentially localized STAT3 proteins in the nucleus and mitochondria cooperate to promote RGC axon regeneration.

Mitochondrial STAT3 Increases Cellular ATP Levels and Complex IV Activity: Contribution of Mitochondrial Electron Transport Chain to Regeneration

Our data indicate that mitochondrial STAT3 has facilitative roles in enhancing RGC axon regeneration, but the underlying mechanism(s) is not known. In non-neuronal cells, mitochondrial STAT3 has been shown to enhance electron transport chain (ETC) complex functions and oxidative phosphorylation (OXPHOS) efficiency (Szczepanek et al., 2011; Wegrzyn et al., 2009). Given that mitochondrial ATP production is significantly compromised in injured neurons, and axon extension requires substantial energy (Mattson, 2007), it is plausible that the improved regeneration seen after expression of STAT3mts and STAT3ca might be due to its ability to enhance mitochondrial bioenergetics in injured neurons. While ATP is generated primarily in the mitochondria via ETC, under certain proliferative states (i.e., during retinal development or tumors), cells can rely mostly on glycolysis to produce ATP (Agathocleous et al., 2012). To first examine the extent to which the ETC contributes to axon regeneration, we assessed RGC axon regeneration in cytochrome *c* oxidase (COX)-deficient mice (Fukui et al., 2007). The *cox10* gene encodes haem A farnesyl transferase, necessary for the assembly of COX (Mogi et al., 1994), the terminal complex of the ETC. In *Cox10*-ablated cells, COX is unstable and rapidly degraded, leading to defects in mitochondrial ATP production (Fukui et al., 2007). C*ox10*$^{f/f}$ mice received intravitreal AAV-Cre injection (Figure S3A) followed by optic nerve crush/AAV-CNTF injection 8 weeks later. Wild-type animals receiving AAV-CNTF showed significant axon regeneration. In contrast, *Cox10* KO animals showed markedly reduced regeneration (Figures S3B and S3C). Interestingly, RGC survival after crush in the *Cox10* KO-mice was similar to the WT mice (Figure S3D), indicating that the ETC requirements for promoting RGC survival and axon regeneration are different. To directly assess the effects of STAT3 expression on mitochondrial functions, we measured the levels of intracellular ATP in WT cortical neurons and observed that expression of STAT3mts (Figures S4A and S4B) leads to significantly higher levels of ATP compared to the control (Figure S4C). We also observed that STAT3mts expression in cortical neurons significantly increases mitochondrial membrane potential (i.e., an indicator of mitochondrial function) (Figure S4D). Additionally, we measured the levels of ETC complex activity and observed that complex IV (but not complex I) activity was significantly higher in STAT3mts group compared to the control (Figures S4E and S4F). These data indicate that mitochondrial ETC is critical for axon regeneration and STAT3 targeted to mitochondria enhances mitochondrial energetics in CNS neurons.

MEK Promotes STAT3 Phosphorylation at S727 and Enhances Expression of STAT3-Induced Genes in CNS Neurons

In addition to STAT3, CNTF also induces activation of ERK, the primary downstream target of MEK (Figure S1). We reasoned that MEK/ERK may enhance transcriptional and mitochondrial STAT3 functions and support regeneration. To test this, we injected AAV expressing the constitutively active form of MEK (MEKca) (Table S1) (Boehm et al., 2007) and observed that this alone results in an increase in the level of pSTAT3(S727), but not pSTAT3(Y705) in the retina (Figure S5A). In retinas, we observed a marked increase in the levels of pERK and pSTAT3(S727) caused by AAV-MEKca in RGCs (Figures S5B–S5D). Next, we examined the effects of MEKca overexpression on the level of STAT3-target gene transcripts. Among the major STAT3 target genes examined (Figure S5F), STAT3ca expression resulted in moderate upregulation of *Ccdkn1a*, *Socs1*, *Socs3*, *Irf1*, and *Atf3*. STAT3wt did not significantly change gene expression levels compared to GFP control, except for *Socs3* (data not shown). Co-expression of MEKca with STAT3ca significantly enhanced expression of each of these genes except for ATF3, compared to STAT3ca alone. These data demonstrate that MEKca promotes phosphorylation of STAT3 (S727) and further enhances expression of STAT3-induced genes in CNS neurons.

MEK Enhances STAT3-Mediated Axon Regeneration

Given its ability to modulate STAT3 at multiple levels, we next tested the effect of MEKca on RGC axon regeneration in the presence of STAT3ca expression. Consistent with the previous study (Pernet et al., 2005), AAV-MEKca alone enhanced RGC survival, but did not significantly enhance regeneration (Figures 4A, 4B, 4D, and 4E). However, co-injection of AAV-MEKca with AAV-STAT3ca markedly increases regeneration compared to AAV-STAT3ca alone (Figures 4A and 4B). Co-injection of AAV-MEKca with AAV-STAT3wt led to a slight increase in regeneration, albeit much lower than the MEKca+STAT3ca group (Figure 4B). Four weeks post-injury, MEKca + STAT3ca treatment led to a 6-fold increase in axon numbers at 1 mm from the lesion site compared to the STAT3ca alone group (Figure 4B). Injection of AAV-MEKca led to transduction of ~70% of RGCs (Figure 4C). In the combined group, nearly all of the AAV-STAT3ca transduced RGCs (i.e., ~60% of RGCs) are also transduced by AAV-MEKca (data not shown). Whole-mount retinal immunohistochemistry shows a similar number of surviving RGCs in the MEKca-alone group compared to the MEKca/STAT3ca-combined group (Figures 4D and 4E).

STAT3/MEK with *Pten*-Deletion Effects on Regenerating RGC Axon Number and Length

Deletion of *Pten* promotes RGC axon regeneration (Park et al., 2008). This regeneration does not rely on STAT3 or B-raf (a major upstream activator of MEK) (O'Donovan et al., 2014; Sun et al., 2011), but depends on Akt/mTOR activation (Park et al., 2008; Sun et al., 2011). Since regeneration by *Pten* deletion involves distinct molecules, we next examined the extent of regeneration after co-overexpressing STAT3ca and MEKca in PTEN KO-neurons. *Pten*$^{f/f}$ mice received an AAV cocktail containing AAV-Cre, AAV-STAT3ca, and AAV-MEKca. Two weeks after AAV injection, animals received optic nerve crush. *Pten* deletion alone promoted axon regeneration. Co-treatment of *Pten* deletion with either MEKca or STAT3ca modestly increased regeneration. Mice receiving the triple AAV treatment (i.e., AAV-Cre, AAV-STAT3ca, and AAV-MEKca) showed massive axon regeneration

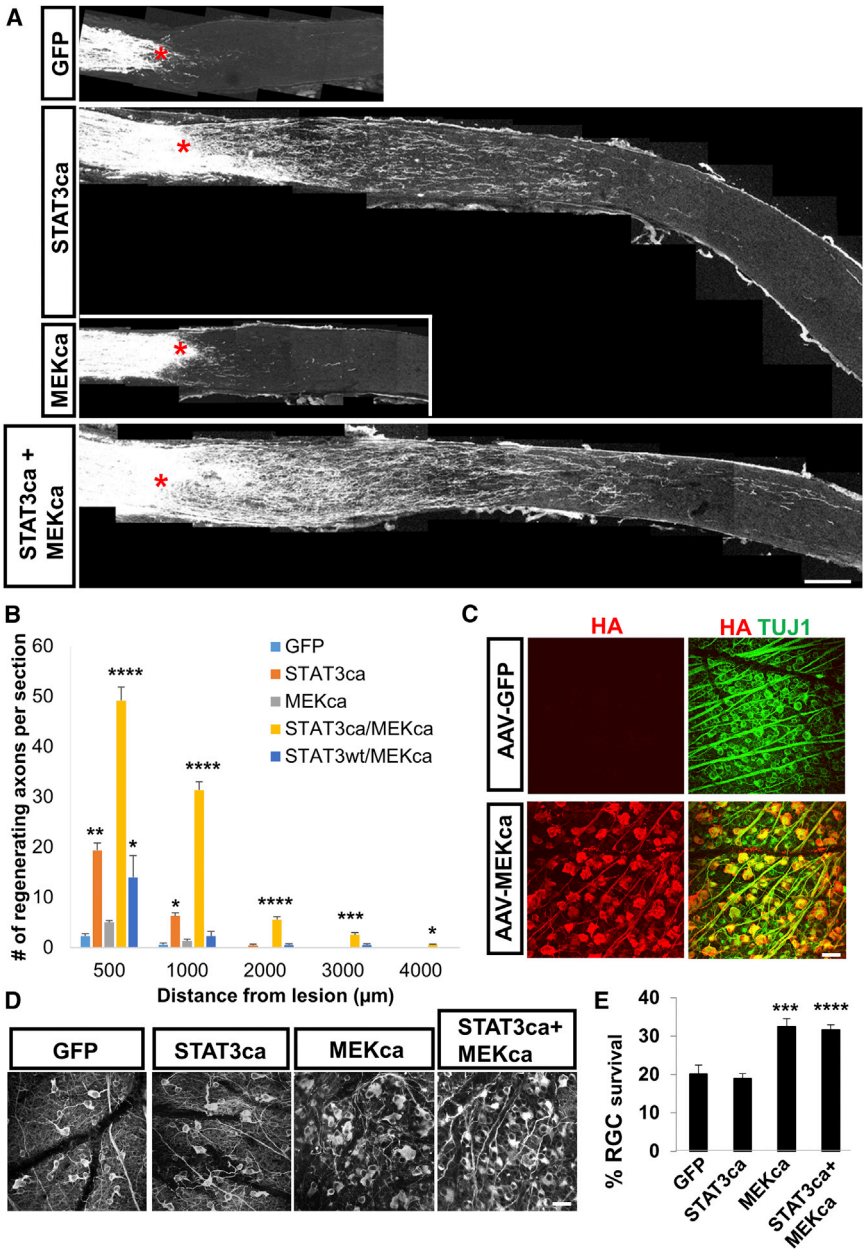

Figure 4. MEK Enhances STAT3-Mediated Axon Regeneration

(A) Representative optic nerve sections showing the degree of axon regeneration 4 weeks after injury in animals treated with either AAV-GFP, AAV-STAT3ca or AAV-MEKca alone, or AAV-STAT3ca/AAV-MEKca. Axons are labeled anterogradely with CTB. Red asterisks, lesion site. Scale bar, 100 μm.

(B) Quantification of CTB-labeled regenerating axons in the various animal groups. n = 4–6 animals/group. *p < 0.05, **p < 0.01, ***p < 0.001, ****p < 0.0001 compared to the "GFP" control group using two-way repeated-measures ANOVA followed by Bonferroni post-test.

(C) Whole-mount retinal immunohistochemistry showing transduction efficacy of the AAV-MEKca. Adult mice received AAV injection, and retinas were removed 2 weeks post-injection. Approximately 70% of RGCs are transduced by the AAV-MEKca as evident by the expression of HA (HA-MEKca) (red) in TUJ1^{+} RGCs (green). Scale bar, 20 μm.

(D) Representative retinal whole-mount images with TUJ1 staining at 4 weeks post-injury in animals subjected to either AAV-GFP, AAV-STAT3ca, or AAV-MEKca alone or combined. Scale bar, 20 μm.

(E) Quantification of RGC survival. Values are represented as the percentage of the contralateral uninjured retina. n = 6 animals/group. ***p < 0.001, ****p < 0.0001 compared to the "GFP" control group using Bonferroni post-test.

See also Figures S5 and S6 and Table S1.

(Figures 5A and 5B). Single or double AAV-treated animals had only a few regenerating axons near the optic chiasm (i.e., 4–5 mm from the optic disc). In comparison, a large number of axons reached the chiasm in the triple AAV-mice (Figures 5A and 5B). Consistent with the single AAV injections, this triple AAV caused Cre expression in the majority of RGCs (~90%) whereas ~70% and 60% of RGCs expressed MEKca and STAT3ca, respectively. We also observed that Cre-expressing RGCs also expressed both STAT3ca and HA (i.e., tag for MEKca) (Figures 5C and 5D). We also used tissue clearing and whole nerve imaging for analysis of axonal trajectories (Luo et al., 2014; Yungher et al., 2015). Three-dimensional examination in the cleared optic nerve shows that the degree of axon turning (i.e., U-turns) is similar among the animal groups, indicating that the higher number of axons distally near the chiasm in the triple AAV-mice is unlikely to be due to differences in axon navigation (Figures S6A and S6B). Analysis of RGC survival showed similar RGC numbers among all groups (Figure S6C). These data demonstrate that simultaneously modulating phosphatase and tensin homolog (PTEN), STAT3, and MEK in neurons increase both the number of regenerating axons and the speed at which they extend when compared to single or double treatments.

To further assess the extent of RGC axon regeneration, we examined regeneration in the cleared, whole brains (Figures 6A and 6B; Movie S1). Four to five weeks post-injury, regenerating axons exit the optic chiasm and continue to extend extensively into the brain. Various growth pattern are seen with axons making turns and arbors within the brain (Figures S6D–S6G). No regenerating axons are seen in the brain of control animals receiving AAV-GFP (n = 8; Figures S6H and S6I). To assess the progression of regeneration, animals were analyzed 10 weeks after injury. Extensive axon regeneration was seen in the brain as evident in the 3D projection and individual brain slices from

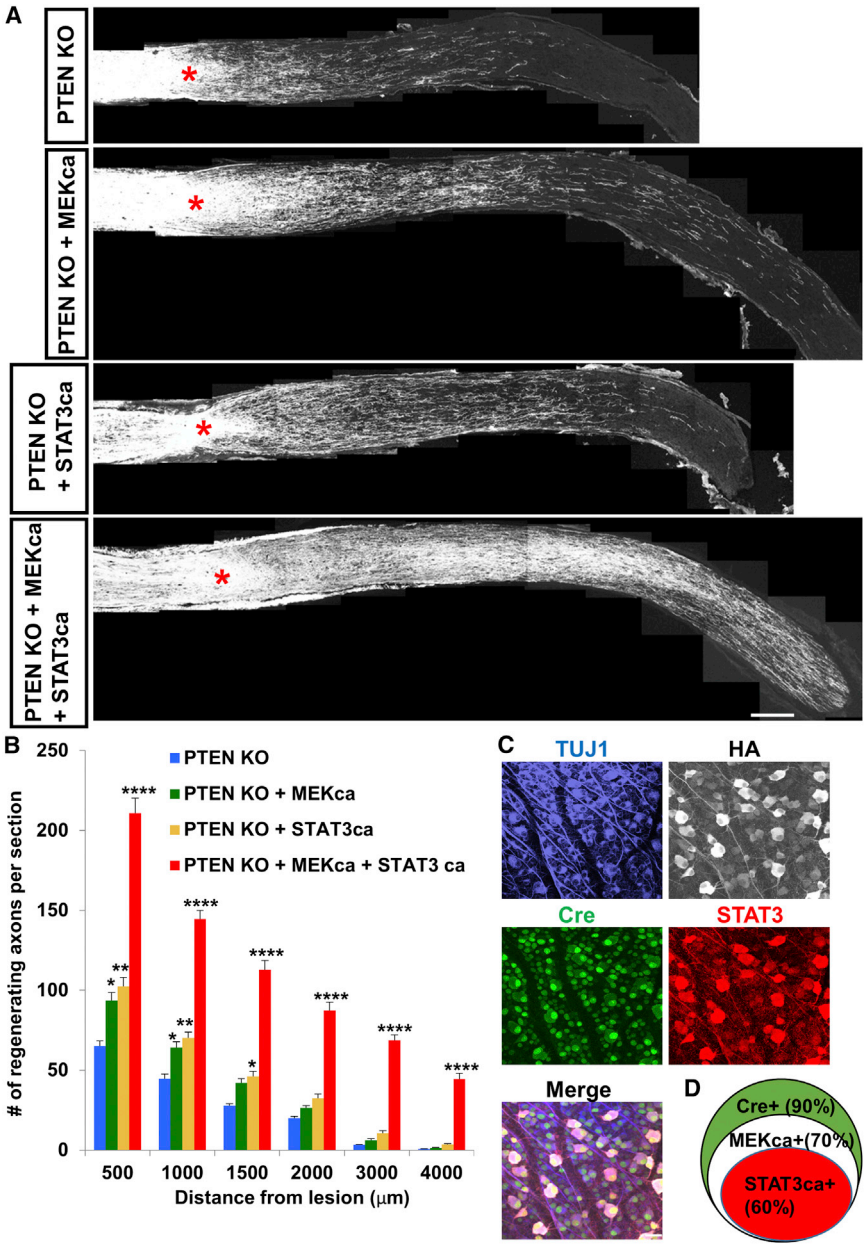

Figure 5. Simultaneously Modulating PTEN, STAT3, and MEK in RGCs Results in Extensive Axon Regeneration

(A) Representative optic nerve sections showing the degree of axon regeneration 4 weeks after injury in *Pten*$^{f/f}$ animals treated with either AAV-Cre alone, AAV-Cre/AAV-MEKca or AAV-Cre/AAV-STAT3ca, or all three AAV together (i.e., AAV-Cre/AAV-STAT3ca/AAV-MEKca). Axons are labeled anterogradely with CTB. Red asterisks, lesion site. Scale bar, 100 μm.

(B) Quantification of CTB-labeled regenerating axons in the various animal groups. n = 6–7 animals/group. *p < 0.05, **p < 0.01, ****p < 0.0001 compared to the "PTEN KO" group using two-way repeated-measures ANOVA followed by Bonferroni post-test.

(C) Whole-mount retinal staining showing AAV transduction efficacy after injection of the triple AAV mix (AAV-Cre, AAV-MEKca, and AAV-STAT3ca) shown by the expression of Cre (green), STAT3 (red), and HA (i.e., tag for MEKca) (white) in TUJ1^{+} RGCs (blue). Adult mice received AAV injection, and retinas were removed 2 weeks post-injection. Scale bar, 20 μm.

(D) Euler diagram showing the percentages of RGC transduction by each AAV and the co-transduction levels.

See also Movies S1, S2, and S3.

the whole brain imaging (Figures 6C–6E; Movies S2 and S3). Consistent with previous studies demonstrating axon misguidance, many axons grew aberrantly throughout the brain (Luo et al., 2013; Pernet et al., 2013a) (Figures 6C–6E; Movies S2 and S3).

STAT3/MEK with *Pten*-Deletion Effects on Axon Sprouting in the Corticospinal Tract

In addition to axon regeneration, which typically refers to re-extension of injured axons, another form of axon remodeling that also contributes significantly to functional recovery after injury, is collateral sprouting of spared, uninjured axons (Tuszynski and Steward, 2012). It has been previously shown that *Pten* deletion or STAT3wt overexpression each promotes axonal sprouting to some degree after spinal cord injury (SCI) (Lang et al., 2013; Lee et al., 2014; Liu et al., 2010). Thus we examined whether the triple AAV treatment synergistically promotes extensive sprouting of uninjured axons after SCI. To this end, we assessed the degree of sprouting of corticospinal tract (CST) neurons after unilateral pyramidotomy (Figure 7A). *Pten*$^{f/f}$*;R26-tdTomato* mice received intracortical injection of AAV-Cre alone or AAV-Cre together with AAV-STAT3ca and AAV-MEKca at 1 week prior to injury. Two additional groups included were (1) *R26-tdTomato* receiving AAV-Cre injection (WT group), and (2) *R26-tdTomato* receiving AAV-Cre, AAV-STAT3ca, and AAV-MEKca. The completeness of lesion was assessed by the degree of loss of PKCγ immunostaining in the lesioned CST tract (Lee et al., 2014). The lesion resulted in essentially complete loss of PKCγ, confirming the severity of pyramidotomy (Figure S7A). At 4 weeks after injury, deletion of *Pten* alone elicited a significant increase in contralateral sprouting of CST axons (i.e., tdTomato^{+} axons) from the intact side (Figures 7B and 7C). Co-treatment with AAV-STAT3ca and AAV-MEKca also enhanced axonal sprouting to some degree. Strikingly, we observed extensive axonal sprouting in animals subjected to the triple AAV (Figures 7B and 7C). Immunohistochemical analysis shows that many CST neurons were

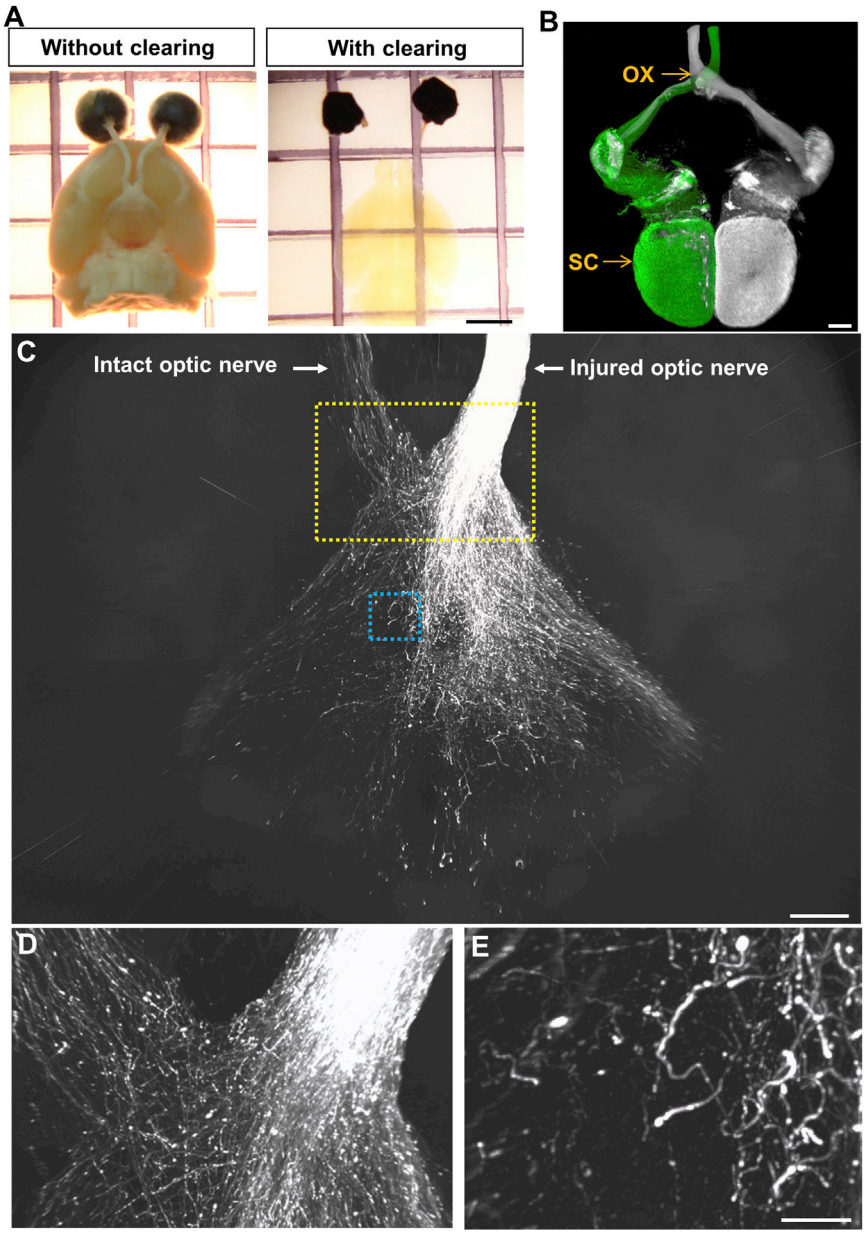

Figure 6. Whole Brain Imaging Reveals Extensive RGC Axon Regeneration following the Triple AAV Treatment

(A) Mouse brains with or without the tissue clearing procedure. Scale bar, 2 mm.

(B) Dorsal view of a cleared brain of uninjured mouse injected with CTB555 (pseudo-colored in white) and CTB488 in the left and right eyes, respectively, showing the entire trajectories of RGC axons from each eye. Tissues were processed 3 days after CTB injection. Scale bar, 500 μm.

(C) Image from axonal projection in the whole, cleared brain of a triple AAV-treated animal 10 weeks after injury. Scale bar, 500 μm.

(D) Higher magnification of the yellow boxed area in (C).

(E) Higher magnification of the blue boxed area in (C). CTB^+ axons grow beyond the optic chiasm and continue to extend to the intact optic nerve or into the brain. OX, optic chiasm; SC, superior colliculus. Scale bar, 50 μm.

See also Movies S1, S2, and S3.

transduced by all three AAV types as evidenced by the concomitant tdTomato, STAT3, and HA (i.e., tag for MEKca) immunoreactivity in the same neurons (Figure S7B). The total numbers of tdTomato-labeled axons in the brainstem at the level of the medullary pyramid were similar among the different animal groups (Figures S7C and S7D). These data demonstrate markedly improved axonal sprouting in injured spinal cord after targeting STAT3 and MEK in *Pten*-deleted animals.

DISCUSSION

Although significant progress has been made in identifying genetic factors involved in axon regeneration failure (Benowitz and Yin, 2007; Cho and Cavalli, 2014; Di Giovanni and Rathore, 2012; Gobrecht et al., 2014; Hammarlund and Jin, 2014; Jiao et al., 2005; Moore and Goldberg, 2011; Omura et al., 2015; Parikh et al., 2011; Planchamp et al., 2008; Saijilafu et al., 2013; Watkins et al., 2013), our understanding of this process remains incomplete. Even with some "fruitful" strategies so far, the number of regrowing axons beyond the lesion site and the extent to which these axons reach their targets remain generally low in adult mammals. One gene consistently implicated in axonal regeneration, in a variety of neuronal types, is *Stat3*. The mechanisms underlying the ability of STAT3 to promote regeneration, however, remain incompletely understood. This is reflected by the fact that merely overexpressing STAT3 in neurons yields limited axon regeneration in vivo. Our study not only extends the previous findings demonstrating mitochondrial presence of STAT3, but also provides direct in vivo evidence of site-specific STAT3 functions in coordinating CNS axon regeneration. Moreover, our results show that MEK is a critical factor that modulates STAT3's phosphorylation status, localization, and functions in RGCs and cortical neurons. The strong regeneration phenotypes that we see, particularly in the STAT3ca and MEKca combined animals, point to the importance of appropriately locating and activating STAT3 through MEK.

Previous studies using combinatorial approaches including *Pten* KO mice with $CNTF^{12,42}$ or b-raf (O'Donovan et al., 2014) (an upstream regulator of MEK) also promoted long distance RGC axon regeneration (Luo et al., 2013; Sun et al., 2011), but the number of regenerating axons in these past studies dropped

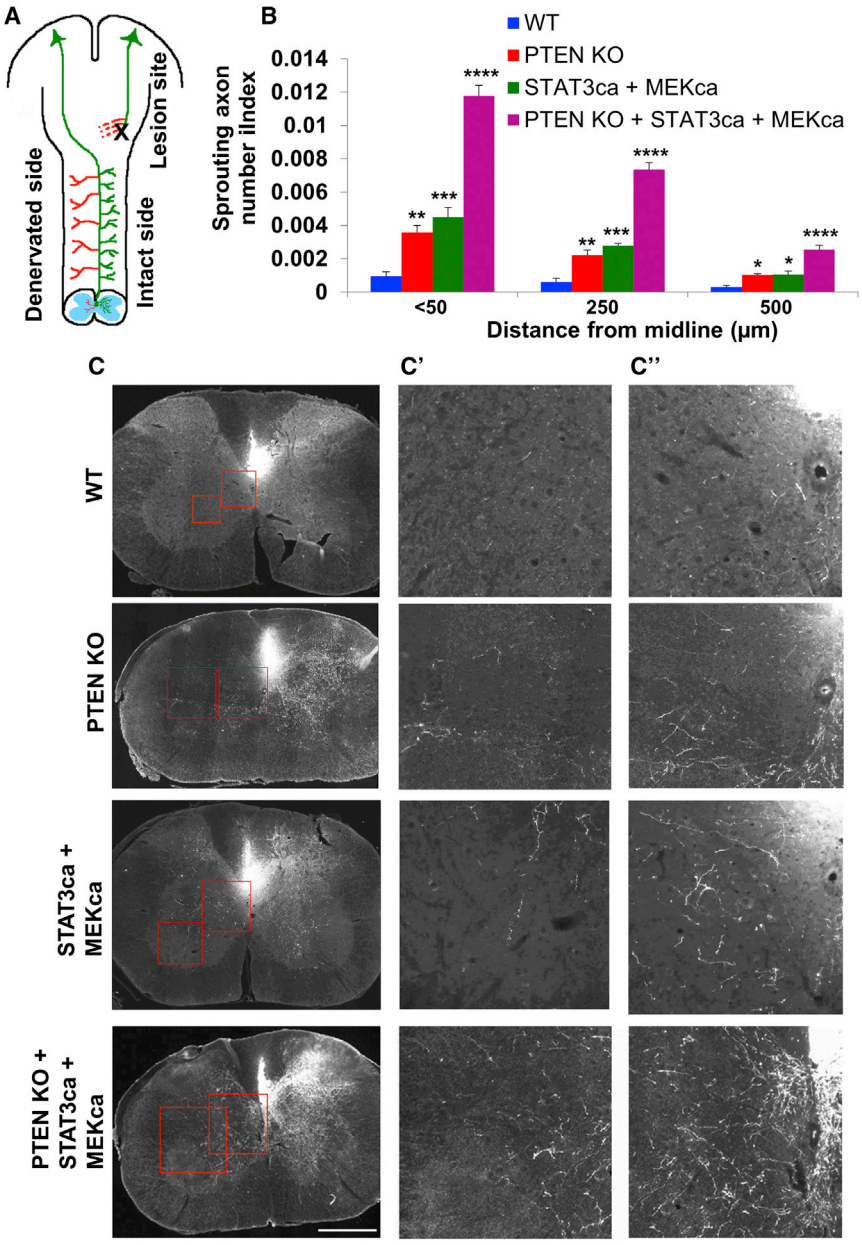

Figure 7. Modulation of PTEN, STAT3, and MEK Results in Extensive CST Sprouting after SCI

(A) Schematic of pyramidotomy model. Corticospinal tract axons (green) originating from the motor cortex are unilaterally transected. Intracortical injection of AAVs into the contralateral brain side allows the examination of treatment effects on axonal sprouting of intact nerves (red).

(B) Quantifications of tdTomato$^+$ crossing axons counted at <50, 250, and 500 μm lateral to the midline in the wild-type control ("WT"), single ("PTEN KO"), double ("STAT3ca + MEKca"), and triple AAV ("PTEN KO + STAT3ca + MEKca") animal groups normalized against the numbers of total labeled CST axons in the medulla. n = 5–6 animals/group. *p < 0.05, **p < 0.01, ***p < 0.001, ****p < 0.0001 compared to the WT group using two-way repeated-measures ANOVA followed by Bonferroni post-test.

(C) Representative of C5 coronal sections in low magnification. High magnification of the boxed regions are shown in (C′) (lateral region) and (C″) (midline region) of the single, double, and triple AAV animal groups. Scale bar, 500 μm.

See also Figure S7.

significantly with distances from the retina, with only a few RGC axons reaching the brain. In contrast, in the triple AAV mice used in this study, hundreds of axons extended into the brain and continued to elongate long distances, densely populating the brain. The same manipulations in CST neurons led to extensive collateral sprouting after SCI.

Recent studies have demonstrated STAT3′s versatile ability to induce cell proliferation and axon growth by acting outside the nucleus, a function that is regulated by phosphorylation. However, whether such a mechanism exists in post-mitotic CNS neurons remained undetermined. We show that STAT3 proteins are phosphorylated at both the tyrosine and serine residues in adult RGCs in response to CNTF. Further, we show that the level of pSTAT3(S727) is increased in mitochondria after CNTF stimulation in a MEK-dependent manner. Thus, our study is in agreement with previous studies demonstrating mitochondrial accumulation of STAT3 in different cell lines (Gough et al., 2009; Wegrzyn et al., 2009; Zhou and Too, 2011). Specifically, others have demonstrated that nerve growth factor (NGF) causes STAT3 phosphorylation exclusively on S727 and promotes mitochondrial translocation, and it is the mitochondrial (not the nuclear) STAT3 that mediates NGF's growth-promoting effects (Zhou and Too, 2011). It has also been demonstrated that cytoplasmic STAT3 is responsible for CNTF's axon growth promoting effects in cultured embryonic neurons (Selvaraj et al., 2012). Thus, while our study is in line with these previous studies describing STAT3′s non-nuclear functions contributing to axon growth, our results also demonstrate the indispensable role of the transcriptional functions of STAT3 in adult CNS axon regeneration. Our results demonstrating a requirement for STAT3′s transcriptional functions, in contrast to being nonessential in embryonic neurons (Selvaraj et al., 2012), suggest that neurons may acquire a reliance on STAT3′s transcription activity to induce axon growth over the course of development. On the other hand, embryonic neurons are perhaps equipped with more versatile and flexible sets of transcription factors that can be activated to induce axon growth in the absence of STAT3′s transcriptional regulation. Regeneration of RGC axons in zebrafish, a

regeneration-competent species, also involves JAK/STAT, but SOCS3 that normally inhibits STAT3′s transcriptional activity did not block regeneration (Elsaeidi et al., 2014). Whether any particular or all of STAT3′s versatile actions contribute in the regeneration-competent species remains unknown. Another notable finding in our study is that although mitochondrial STAT3 alone is insufficient to promote regeneration, it further improves regeneration when the levels of nuclear active STAT3 are increased. Overall, our data indicate that distinctly distributed STAT3 in the nucleus and mitochondria modulate synergistic nuclear transcription and yet undefined mitochondrial mechanisms, and this bi-functionality of STAT3 induces optimal CNS axon regeneration. Interestingly, mitochondria STAT3 was also shown to facilitate the production of reactive oxygen species (ROS) and this allowed neurite extension (Zhou and Too, 2011), suggesting that STAT3 may modulate different aspects of mitochondrial functions that coordinately improve regeneration.

Several studies have demonstrated that CNTF and STAT3 modulate mitochondrial bioenergetics; CNTF enhances respiratory capacity in sensory neurons (Chowdhury et al., 2014). STAT3 prevents a decrease in complex I activity under ischemia (Szczepanek et al., 2011). Furthermore, STAT3-ablated cells exhibit defective ATP production (Sarafian et al., 2010; Wegrzyn et al., 2009). However, the precise mechanisms by which STAT3 locally modulates mitochondrial functions are currently unknown. Our study shows that STAT3 localizes to mitochondrial inner membrane in response to CNTF, and STAT3mts enhances cellular ATP levels, membrane potential, and complex IV activity. Since *Cox10*-ablated RGCs have significantly reduced axon regeneration, improved regeneration seen after expression of STAT3mts could be due, at least in part, to its ability to maintain or enhance mitochondrial ATP production following injury. We also observed that *Cox10* deletion reduces axon regeneration in PTEN-ablated cells (data now shown), underlining the idea that the effects of ETC might be a general phenomenon for CNS axon regeneration.

It is notable that MEKca leads to considerable regeneration when it is combined with STAT3ca. MEK/ERK pathway is known to activate or silence many different proteins downstream and thus controls many distinct cellular processes including gene transcription, translation, as well as protein transport. Our data indicate that MEK-dependent localization of STAT3 to mitochondria could be one mechanism by which MEK facilitates STAT3-induced axon regeneration. Recently, it was demonstrated that retrogradely transported ERK activates histone acetyltransferases including p300/CBP-associated factor in the cell body, leading to enhanced acetylation and expression of several regeneration-associated genes (Puttagunta et al., 2014). Similarly, axon injury causes retrograde transport of axonal STAT3 to the cell body (Ben-Yaakov et al., 2012). Thus, in addition to acting downstream of growth factors at the soma, STAT3 and ERK may represent a complementary "dual" injury signal that collectively links the axon and soma response. In sum, our study extends STAT3′s diverse abilities to function in distinct cellular regions in mature CNS neurons but also indicates that in mature neurons, STAT3′s transcription regulation is at the "center" of growth promotion with mitochondrial STAT3 likely playing facilitative roles, overall providing a more clear idea about how STAT3 could be manipulated to induce CNS axon regeneration. Delineating STAT3′s divergent functions and understanding how these processes are regulated may lead to more targeted therapy for promoting functional axon regrowth.

EXPERIMENTAL PROCEDURES

Further details of methods and materials are provided in the Supplemental Experimental Procedures.

Animals

All experimental procedures were performed in compliance with protocols approved by the Institutional Animal Care and Use Committee (IACUC) at University of Miami. Animals used are C57BL/6J, *Pten*$^{f/f}$ (stock number 006440; Jackson Laboratory), *Stat3*$^{f/f}$ mice (stock number 016923; Jackson Laboratory), *R26 loxP-stop-loxP-tdTomato* (*R26-tdTomato*; a generous gift from Dr. Fan Wang, Duke University), *Cox10*$^{f/f}$ (Fukui et al., 2007) and *Pten*$^{f/f}$*;R26-tdTomato, Stat3*$^{f/f}$*;R26-tdTomato.* For all surgical procedures, mice were anaesthetized with ketamine and xylazine, and buprenorphine (0.05 mg/kg, Bedford Lab) was administrated as post-operative analgesic. At least five animals were used for each groups in the axon regeneration and RGC survival experiment unless indicated otherwise. The precise animal numbers are also indicated in the figure legends.

Optic Nerve Crush

For optic nerve crush injury, the optic nerve was exposed intraorbitally and crushed with jeweler's forceps (Dumont #5, Roboz) for 10 s ~1 mm behind the optic disc.

Intravitreal Injection

Female or male mice (5- to 7-week-old) received unilateral AAV injection. For each intravitreal injection, a glass micropipette was inserted into the peripheral retina, just behind the ora serrata, and was deliberately angled to avoid damage to the lens. To anterogradely label regenerating RGC axons, animals received intravitreal injection of 2 μl of cholera toxin β subunit (CTB)-Alexa 555 or CTB-Alexa 488 (2 μg/μl, Invitrogen) with a Hamilton syringe (Hamilton) at 2–5 days before euthanasia.

Statistics

GraphPad Prism (GraphPad Software) was used for statistical analyses. Data were analyzed using ANOVA and the Bonferroni within-groups comparison with additional testing using Dunnett's test or Student's t test. Values of $p < 0.05$ were considered significant. All error bars indicate SEM unless indicated otherwise in the figure legends.

SUPPLEMENTAL INFORMATION

Supplemental Information includes Supplemental Experimental Procedures, seven figures, one table, and three movies and can be found with this article online at http://dx.doi.org/10.1016/j.celrep.2016.03.029.

AUTHOR CONTRIBUTIONS

K.K.P. supervised the project. X.L. and K.K.P. planned and performed experiments, analyzed data, and wrote the manuscript. C.T.M. and F.D. provided the transgenic mice. M.R., D.-H.L., B.J.Y., E.R.B., S.M., and K.A.T. performed the experiments. J.L.B., V.P.L., and J.K.L. advised and analyzed the data.

ACKNOWLEDGMENTS

This work was supported by grants from the National Eye Institute (NEI) 1R01EY022961-01 (to K.K.P.), National Institute of Neurological Disorders and Stroke (NINDS) R01NS009923-43 (to K.K.P.), the Eunice Kennedy Shriver National Institute of Child Health and Human Development (NICHD) R01HD057632 (to V.P.L. and J.L.B.), 5R01EY010804 (to C.T.M.), 5R01NS079965 (to C.T.M.), U.S. Army W81XWH-05-1-0061 (to K.K.P.),

W81XWH-12-1-0319 (to K.K.P.), Ziegler Foundation (to K.K.P.), Pew Charitable Trust (to K.K.P.), Craig H. Neilsen Foundation (to K.K.P.), and the Buoniconti Fund (to K.K.P., V.P.L., J.K.L., and J.L.B.). We thank Aline-Ohashi Hida for her help with *Cox10*$^{f/f}$ mice, Melissa Carballosa-Gautam at the Miami Project to Cure Paralysis Imaging Core, Margaret Rebecca Bates and Vania Wolff Almeida at the University of Miami Electron Microscopy Core, Yadira Salgueiro in the K.K.P. lab and Pingping Jia at the University of Miami Viral Vector Core.

Received: July 16, 2015
Revised: December 21, 2015
Accepted: March 7, 2016
Published: March 31, 2016

REFERENCES

Agathocleous, M., Love, N.K., Randlett, O., Harris, J.J., Liu, J., Murray, A.J., and Harris, W.A. (2012). Metabolic differentiation in the embryonic retina. Nat. Cell Biol. *14*, 859–864.

Bareyre, F.M., Garzorz, N., Lang, C., Misgeld, T., Büning, H., and Kerschensteiner, M. (2011). In vivo imaging reveals a phase-specific role of STAT3 during central and peripheral nervous system axon regeneration. Proc. Natl. Acad. Sci. USA *108*, 6282–6287.

Ben-Yaakov, K., Dagan, S.Y., Segal-Ruder, Y., Shalem, O., Vuppalanchi, D., Willis, D.E., Yudin, D., Rishal, I., Rother, F., Bader, M., et al. (2012). Axonal transcription factors signal retrogradely in lesioned peripheral nerve. EMBO J. *31*, 1350–1363.

Benowitz, L.I., and Yin, Y. (2007). Combinatorial treatments for promoting axon regeneration in the CNS: strategies for overcoming inhibitory signals and activating neurons' intrinsic growth state. Dev. Neurobiol. *67*, 1148–1165.

Boehm, J.S., Zhao, J.J., Yao, J., Kim, S.Y., Firestein, R., Dunn, I.F., Sjostrom, S.K., Garraway, L.A., Weremowicz, S., Richardson, A.L., et al. (2007). Integrative genomic approaches identify IKBKE as a breast cancer oncogene. Cell *129*, 1065–1079.

Bromberg, J.F., Horvath, C.M., Besser, D., Lathem, W.W., and Darnell, J.E., Jr. (1998). Stat3 activation is required for cellular transformation by v-src. Mol. Cell. Biol. *18*, 2553–2558.

Bromberg, J.F., Wrzeszczynska, M.H., Devgan, G., Zhao, Y., Pestell, R.G., Albanese, C., and Darnell, J.E., Jr. (1999). Stat3 as an oncogene. Cell *98*, 295–303.

Cafferty, W.B., Gardiner, N.J., Das, P., Qiu, J., McMahon, S.B., and Thompson, S.W. (2004). Conditioning injury-induced spinal axon regeneration fails in interleukin-6 knock-out mice. J. Neurosci. *24*, 4432–4443.

Cao, Z., Gao, Y., Bryson, J.B., Hou, J., Chaudhry, N., Siddiq, M., Martinez, J., Spencer, T., Carmel, J., Hart, R.B., and Filbin, M.T. (2006). The cytokine interleukin-6 is sufficient but not necessary to mimic the peripheral conditioning lesion effect on axonal growth. J. Neurosci. *26*, 5565–5573.

Case, L.C., and Tessier-Lavigne, M. (2005). Regeneration of the adult central nervous system. Curr. Biol. *15*, R749–R753.

Cho, Y., and Cavalli, V. (2014). HDAC signaling in neuronal development and axon regeneration. Curr. Opin. Neurobiol. *27*, 118–126.

Chowdhury, S.R., Saleh, A., Akude, E., Smith, D.R., Morrow, D., Tessler, L., Calcutt, N.A., and Fernyhough, P. (2014). Ciliary neurotrophic factor reverses aberrant mitochondrial bioenergetics through the JAK/STAT pathway in cultured sensory neurons derived from streptozotocin-induced diabetic rodents. Cell. Mol. Neurobiol. *34*, 643–649.

Cregg, J.M., DePaul, M.A., Filous, A.R., Lang, B.T., Tran, A., and Silver, J. (2014). Functional regeneration beyond the glial scar. Exp. Neurol. *253*, 197–207.

Di Giovanni, S., and Rathore, K. (2012). p53-Dependent pathways in neurite outgrowth and axonal regeneration. Cell Tissue Res. *349*, 87–95.

Elsaeidi, F., Bemben, M.A., Zhao, X.F., and Goldman, D. (2014). Jak/Stat signaling stimulates zebrafish optic nerve regeneration and overcomes the inhibitory actions of Socs3 and Sfpq. J. Neurosci. *34*, 2632–2644.

Ernst, M., and Jenkins, B.J. (2004). Acquiring signalling specificity from the cytokine receptor gp130. Trends Genet. *20*, 23–32.

Fukui, H., Diaz, F., Garcia, S., and Moraes, C.T. (2007). Cytochrome c oxidase deficiency in neurons decreases both oxidative stress and amyloid formation in a mouse model of Alzheimer's disease. Proc. Natl. Acad. Sci. USA *104*, 14163–14168.

Gallagher, D., Gutierrez, H., Gavalda, N., O'Keeffe, G., Hay, R., and Davies, A.M. (2007). Nuclear factor-kappaB activation via tyrosine phosphorylation of inhibitor kappaB-alpha is crucial for ciliary neurotrophic factor-promoted neurite growth from developing neurons. J. Neurosci. *27*, 9664–9669.

Gobrecht, P., Leibinger, M., Andreadaki, A., and Fischer, D. (2014). Sustained GSK3 activity markedly facilitates nerve regeneration. Nat. Commun. *5*, 4561.

Gough, D.J., Corlett, A., Schlessinger, K., Wegrzyn, J., Larner, A.C., and Levy, D.E. (2009). Mitochondrial STAT3 supports Ras-dependent oncogenic transformation. Science *324*, 1713–1716.

Hammarlund, M., and Jin, Y. (2014). Axon regeneration in C. elegans. Curr. Opin. Neurobiol. *27*, 199–207.

Horvath, C.M., Wen, Z., and Darnell, J.E., Jr. (1995). A STAT protein domain that determines DNA sequence recognition suggests a novel DNA-binding domain. Genes Dev. *9*, 984–994.

Huebner, E.A., and Strittmatter, S.M. (2009). Axon regeneration in the peripheral and central nervous systems. Results Probl. Cell Differ. *48*, 339–351.

Jiao, J., Huang, X., Feit-Leithman, R.A., Neve, R.L., Snider, W., Dartt, D.A., and Chen, D.F. (2005). Bcl-2 enhances Ca(2+) signaling to support the intrinsic regenerative capacity of CNS axons. EMBO J. *24*, 1068–1078.

Lang, C., Bradley, P.M., Jacobi, A., Kerschensteiner, M., and Bareyre, F.M. (2013). STAT3 promotes corticospinal remodelling and functional recovery after spinal cord injury. EMBO Rep. *14*, 931–937.

Leaver, S.G., Cui, Q., Bernard, O., and Harvey, A.R. (2006). Cooperative effects of bcl-2 and AAV-mediated expression of CNTF on retinal ganglion cell survival and axonal regeneration in adult transgenic mice. Eur. J. Neurosci. *24*, 3323–3332.

Lee, D.H., Luo, X., Yungher, B.J., Bray, E., Lee, J.K., and Park, K.K. (2014). Mammalian target of rapamycin's distinct roles and effectiveness in promoting compensatory axonal sprouting in the injured CNS. J. Neurosci. *34*, 15347–15355.

Leibinger, M., Müller, A., Andreadaki, A., Hauk, T.G., Kirsch, M., and Fischer, D. (2009). Neuroprotective and axon growth-promoting effects following inflammatory stimulation on mature retinal ganglion cells in mice depend on ciliary neurotrophic factor and leukemia inhibitory factor. J. Neurosci. *29*, 14334–14341.

Leibinger, M., Andreadaki, A., Diekmann, H., and Fischer, D. (2013). Neuronal STAT3 activation is essential for CNTF- and inflammatory stimulation-induced CNS axon regeneration. Cell Death Dis. *4*, e805.

Liu, K., Lu, Y., Lee, J.K., Samara, R., Willenberg, R., Sears-Kraxberger, I., Tedeschi, A., Park, K.K., Jin, D., Cai, B., et al. (2010). PTEN deletion enhances the regenerative ability of adult corticospinal neurons. Nat. Neurosci. *13*, 1075–1081.

Luo, X., Salgueiro, Y., Beckerman, S.R., Lemmon, V.P., Tsoulfas, P., and Park, K.K. (2013). Three-dimensional evaluation of retinal ganglion cell axon regeneration and pathfinding in whole mouse tissue after injury. Exp. Neurol. *247*, 653–662.

Luo, X., Yungher, B., and Park, K.K. (2014). Application of tissue clearing and light sheet fluorescence microscopy to assess optic nerve regeneration in unsectioned tissues. Methods Mol. Biol. *1162*, 209–217.

Martell, J.D., Deerinck, T.J., Sancak, Y., Poulos, T.L., Mootha, V.K., Sosinsky, G.E., Ellisman, M.H., and Ting, A.Y. (2012). Engineered ascorbate peroxidase as a genetically encoded reporter for electron microscopy. Nat. Biotechnol. *30*, 1143–1148.

Mattson, M.P. (2007). Mitochondrial regulation of neuronal plasticity. Neurochem. Res. *32*, 707–715.

Mogi, T., Saiki, K., and Anraku, Y. (1994). Biosynthesis and functional role of haem O and haem A. Mol. Microbiol. *14*, 391–398.

Moore, D.L., and Goldberg, J.L. (2011). Multiple transcription factor families regulate axon growth and regeneration. Dev. Neurobiol. *71*, 1186–1211.

Müller, A., Hauk, T.G., Leibinger, M., Marienfeld, R., and Fischer, D. (2009). Exogenous CNTF stimulates axon regeneration of retinal ganglion cells partially via endogenous CNTF. Mol. Cell. Neurosci. *41*, 233–246.

O'Donovan, K.J., Ma, K., Guo, H., Wang, C., Sun, F., Han, S.B., Kim, H., Wong, J.K., Charron, J., Zou, H., et al. (2014). B-RAF kinase drives developmental axon growth and promotes axon regeneration in the injured mature CNS. J. Exp. Med. *211*, 801–814.

Omura, T., Omura, K., Tedeschi, A., Riva, P., Painter, M.W., Rojas, L., Martin, J., Lisi, V., Huebner, E.A., Latremoliere, A., et al. (2015). Robust axonal regeneration occurs in the injured CAST/Ei mouse CNS. Neuron *86*, 1215–1227.

Parikh, P., Hao, Y., Hosseinkhani, M., Patil, S.B., Huntley, G.W., Tessier-Lavigne, M., and Zou, H. (2011). Regeneration of axons in injured spinal cord by activation of bone morphogenetic protein/Smad1 signaling pathway in adult neurons. Proc. Natl. Acad. Sci. USA *108*, E99–E107.

Park, K.K., Liu, K., Hu, Y., Smith, P.D., Wang, C., Cai, B., Xu, B., Connolly, L., Kramvis, I., Sahin, M., and He, Z. (2008). Promoting axon regeneration in the adult CNS by modulation of the PTEN/mTOR pathway. Science *322*, 963–966.

Pellegrino, M.J., and Habecker, B.A. (2013). STAT3 integrates cytokine and neurotrophin signals to promote sympathetic axon regeneration. Mol. Cell. Neurosci. *56*, 272–282.

Pernet, V., Hauswirth, W.W., and Di Polo, A. (2005). Extracellular signal-regulated kinase 1/2 mediates survival, but not axon regeneration, of adult injured central nervous system neurons in vivo. J. Neurochem. *93*, 72–83.

Pernet, V., Joly, S., Dalkara, D., Jordi, N., Schwarz, O., Christ, F., Schaffer, D.V., Flannery, J.G., and Schwab, M.E. (2013a). Long-distance axonal regeneration induced by CNTF gene transfer is impaired by axonal misguidance in the injured adult optic nerve. Neurobiol. Dis. *51*, 202–213.

Pernet, V., Joly, S., Jordi, N., Dalkara, D., Guzik-Kornacka, A., Flannery, J.G., and Schwab, M.E. (2013b). Misguidance and modulation of axonal regeneration by Stat3 and Rho/ROCK signaling in the transparent optic nerve. Cell Death Dis. *4*, e734.

Planchamp, V., Bermel, C., Tönges, L., Ostendorf, T., Kügler, S., Reed, J.C., Kermer, P., Bähr, M., and Lingor, P. (2008). BAG1 promotes axonal outgrowth and regeneration in vivo via Raf-1 and reduction of ROCK activity. Brain *131*, 2606–2619.

Puttagunta, R., Tedeschi, A., Sória, M.G., Hervera, A., Lindner, R., Rathore, K.I., Gaub, P., Joshi, Y., Nguyen, T., Schmandke, A., et al. (2014). PCAF-dependent epigenetic changes promote axonal regeneration in the central nervous system. Nat. Commun. *5*, 3527.

Saijilafu, Z., Zhang, B.Y., and Zhou, F.Q. (2013). Signaling pathways that regulate axon regeneration. Neurosci. Bull. *29*, 411–420.

Saleh, A., Roy Chowdhury, S.K., Smith, D.R., Balakrishnan, S., Tessler, L., Martens, C., Morrow, D., Schartner, E., Frizzi, K.E., Calcutt, N.A., and Fernyhough, P. (2013). Ciliary neurotrophic factor activates NF-κB to enhance mitochondrial bioenergetics and prevent neuropathy in sensory neurons of streptozotocin-induced diabetic rodents. Neuropharmacology *65*, 65–73.

Sarafian, T.A., Montes, C., Imura, T., Qi, J., Coppola, G., Geschwind, D.H., and Sofroniew, M.V. (2010). Disruption of astrocyte STAT3 signaling decreases mitochondrial function and increases oxidative stress in vitro. PLoS ONE *5*, e9532.

Selvaraj, B.T., Frank, N., Bender, F.L., Asan, E., and Sendtner, M. (2012). Local axonal function of STAT3 rescues axon degeneration in the pmn model of motoneuron disease. J. Cell Biol. *199*, 437–451.

Smith, P.D., Sun, F., Park, K.K., Cai, B., Wang, C., Kuwako, K., Martinez-Carrasco, I., Connolly, L., and He, Z. (2009). SOCS3 deletion promotes optic nerve regeneration in vivo. Neuron *64*, 617–623.

Sun, F., and He, Z. (2010). Neuronal intrinsic barriers for axon regeneration in the adult CNS. Curr. Opin. Neurobiol. *20*, 510–518.

Sun, F., Park, K.K., Belin, S., Wang, D., Lu, T., Chen, G., Zhang, K., Yeung, C., Feng, G., Yankner, B.A., and He, Z. (2011). Sustained axon regeneration induced by co-deletion of PTEN and SOCS3. Nature *480*, 372–375.

Szczepanek, K., Chen, Q., Derecka, M., Salloum, F.N., Zhang, Q., Szelag, M., Cichy, J., Kukreja, R.C., Dulak, J., Lesnefsky, E.J., and Larner, A.C. (2011). Mitochondrial-targeted Signal transducer and activator of transcription 3 (STAT3) protects against ischemia-induced changes in the electron transport chain and the generation of reactive oxygen species. J. Biol. Chem. *286*, 29610–29620.

Tammineni, P., Anugula, C., Mohammed, F., Anjaneyulu, M., Larner, A.C., and Sepuri, N.B. (2013). The import of the transcription factor STAT3 into mitochondria depends on GRIM-19, a component of the electron transport chain. J. Biol. Chem. *288*, 4723–4732.

Taniguchi, K., Wu, L.W., Grivennikov, S.I., de Jong, P.R., Lian, I., Yu, F.X., Wang, K., Ho, S.B., Boland, B.S., Chang, J.T., et al. (2015). A gp130-Src-YAP module links inflammation to epithelial regeneration. Nature *519*, 57–62.

Tuszynski, M.H., and Steward, O. (2012). Concepts and methods for the study of axonal regeneration in the CNS. Neuron *74*, 777–791.

Watkins, T.A., Wang, B., Huntwork-Rodriguez, S., Yang, J., Jiang, Z., Eastham-Anderson, J., Modrusan, Z., Kaminker, J.S., Tessier-Lavigne, M., and Lewcock, J.W. (2013). DLK initiates a transcriptional program that couples apoptotic and regenerative responses to axonal injury. Proc. Natl. Acad. Sci. USA *110*, 4039–4044.

Wegrzyn, J., Potla, R., Chwae, Y.J., Sepuri, N.B., Zhang, Q., Koeck, T., Derecka, M., Szczepanek, K., Szelag, M., Gornicka, A., et al. (2009). Function of mitochondrial Stat3 in cellular respiration. Science *323*, 793–797.

Yungher, B.J., Luo, X., Salgueiro, Y., Blackmore, M.G., and Park, K.K. (2015). Viral vector-based improvement of optic nerve regeneration: characterization of individual axons' growth patterns and synaptogenesis in a visual target. Gene Ther. *22*, 811–821.

Zhou, L., and Too, H.P. (2011). Mitochondrial localized STAT3 is involved in NGF induced neurite outgrowth. PLoS ONE *6*, e21680.

Zigmond, R.E. (2011). gp130 cytokines are positive signals triggering changes in gene expression and axon outgrowth in peripheral neurons following injury. Front. Mol. Neurosci. *4*, 62.